Safety Envelope for Load Tolerance and its Application to Fatigue Reliability Design

Haoyu Wang
Graduate Student
Department of Mechanical and Aerospace Engineering,
University of Florida,
Gainesville, FL 32611

Nam H. Kim
Assistant Professor
Department of Mechanical and Aerospace Engineering,
University of Florida,
PO Box 116250,
Gainesville, FL 32611
e-mail: nkim@ufl.edu

Yoon-Jun Kim
Senior Researcher
Technical Center,
Caterpillar Inc.,
PO Box 1875,
Peoria, IL 61656

In this paper, a safety envelope concept for load tolerance is introduced. This shows the capacity of the current design as a future reference for design upgrade, maintenance, and control. The safety envelope is applied to estimate the load tolerance of a structural part with respect to the fatigue reliability. First, the dynamic load history is decomposed into the average value and amplitude, which are modeled as random variables. Second, through fatigue analysis and uncertainty propagation, the reliability is calculated. Last, based on the implicit function evaluation for the reliability, the boundary of the safety envelope is calculated numerically. The effect of different distribution types of random variables is then investigated to identify the conservative envelope. In order to improve the efficiency of searching the boundary, probabilistic sensitivity information is utilized. When the relationship between the safety of the system and the load tolerance is linear or mildly nonlinear, the linear estimation of the safety envelope turns out to be accurate and efficient. During the application of the algorithm, a stochastic response surface of logarithmic fatigue life with respect to the load capacity coefficient is constructed, and the Monte Carlo simulation is utilized to calculate the reliability and its sensitivities.
[DOI: 10.1115/1.2204971]

1 Introduction

Traditionally, structural design under uncertainty treats structural dimensions, shapes, and material properties as uncertainty parameters. These parameters are relatively well controlled, so that their variability is usually small. However, the uncertainty in the applied load is much larger than in others. The variability of the load is often ignored in the design stage because it is difficult to quantify. Without knowing the accurate uncertainty characteristics of inputs, it is dubious to rely on the reliability result of the output. In this paper, a different approach is taken by asking how much load and variability a system can support. The amount of load that a structure can support becomes important information for evaluating the design. Traditional design concerns load capacity by introducing a safety factor, which is supposed to provide a safety margin under the random load conditions. Kwak and Kim [1] proposed a concept of allowable load sets, where deterministic loads are used without considering uncertainties involved in it. In linear static structures, the allowable load set becomes piecewise linear and convex.

In this paper, the idea of the allowable load set is further extended to the fatigue life estimation under uncertainty in the applied dynamic loads using the stochastic response surface technique [2,3] and sensitivity information [4,5]. The dynamic load is parametrized, and the uncertainty of the parameters is modeled as a random variable. Since the problem at hand includes the fatigue life of dynamic systems, it is computationally intensive, without mentioning the reliability analysis. Thus, it is important to calculate uncertainty propagation efficiently. Instead of searching the load tolerance directly, an estimation method using the data at the current load and their sensitivity is proposed. This idea can be further extended to the multi-dimensional case, in which the load tolerance becomes a safety envelope.

With reference to Fig. 1, the analysis procedure can be decomposed into three different levels:

(1) Calculate the fatigue life of the structure when a dynamic load history is provided. In this particular application, a commercial program, FE-SAFE [6], is used to calculate the fatigue life.
(2) Construct the stochastic response surface to calculate the reliability of the fatigue life due to the uncertainty in load parameters.
(3) Predict the load tolerance and construct the safety envelope using the predictor-corrector algorithm.

2 Parametrization of Dynamic Loads

The safety of a structure strongly depends on the assumptions given in the input conditions. Among them, the assumption in the applied load may be the most important factor. Thus, it would not make any sense to analyze and design a structure without considering the variability of the load. The same design can be safe or failed based on input loads. However, input loads are often unknown, especially for dynamic systems. As shown in Fig. 2, dynamic loads are usually complicated and involve uncertainties.

In general the load characteristics from one operator may completely differ from that of others. In order to perform reliability analysis, it is necessary to characterize the uncertainties involved in the inputs. However, the distribution type and parameters of loads are often unknown. As a partial remedy for this difficulty, it is assumed that the representative dynamic load history $f_0(t)$ is available either from experiments or from computer simulations. This dynamic load is decomposed into the average value and amplitude. The parametrization of the dynamic load can then be introduced by changing the average value and amplitude as

$$f(t) = \alpha f_{\text{ave}} + \gamma(f_0(t) - f_{\text{ave}}) \tag{1}$$

where f_{ave} is the average value of $f_0(t)$, and α and γ are the load capacity coefficients (LCC) for the average value and amplitude, respectively. When $\alpha = \gamma = 1$, the applied load is identical to the initial load history. In Eq. (1), α and γ cannot be negative. Equation (1) provides a convenient method of parametrization because only two parameters are involved and the dynamic characteristics of the initial load history can be preserved. Considering that the fatigue life of the structure depends on the average value and

Contributed by the Design Automation Committee of ASME for publication in the JOURNAL OF MECHANICAL DESIGN. Manuscript received September 19, 2005; final manuscript received December 22, 2005. Review conducted by Zissimos P. Mourelatos.

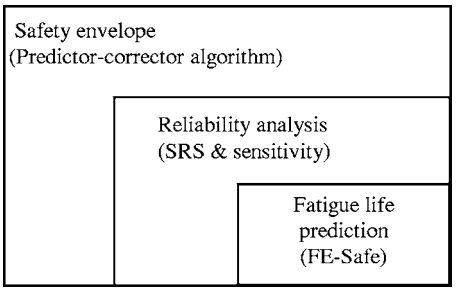

Fig. 1 Analysis procedure of constructing safety envelope

amplitude of dynamic loads, the parametrization in Eq. (1) is also consistent with fatigue analysis.

In reliability analysis, α and γ are considered as random variables that can represent the statistical behavior of the applied dynamic load. In a traditional reliability-based design, variability in parameters is usually modeled by assuming a specific type of random distribution. In practice, however, engineers have some knowledge about the input variables, but the information may not be accurate. In the case of the dynamic load history, for example, the statistical property of the load can be obtained from a histogram of the load. However, it may not be clearly shown whether it is normal or lognormal distribution. In such a case, the engineer can consider both distributions and select the conservative one. In this paper, the effect of different distribution types on the response is investigated by introducing the concept of the conservative distribution type, which provides a safer way to model uncertainties.

3 Fatigue Life Prediction

The computational model is the front loader frame of civil construction equipment. The model consists of about 172,000 finite elements. Dynamic loads are measured at 26 different channels. More than 9000 peak and valleys of dynamic loads are sampled during the 46 min composite working cycle. The procedure of finite element based quasi-static fatigue life prediction [7] is shown in Fig. 3. In the fatigue analysis, a unit static load is first applied per each channel or load degree of freedom to calculate the stress influence coefficient. The stress influence coefficients are multiplied by the dynamic load history to calculate the dynamic stress history.

As illustrated in Fig. 3, by collecting different stress amplitudes at different times using the rain-flow cycle counting technique [8], the fatigue damage is linearly accumulated, as is proposed by Miner [9]. Based on the available material properties and the component's working conditions, the fatigue life of the critical point is evaluated. The stress-life method is used to determine the fatigue

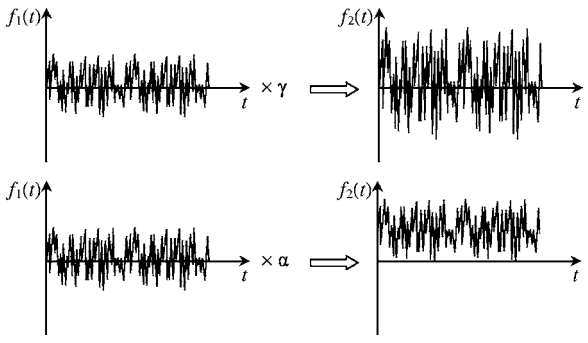

Fig. 2 Parametrization of dynamic loads using the average value and amplitude. This method preserves the fundamental characteristics of the dynamic load history, while it is flexible enough so that the various effects of the dynamic loads can be included.

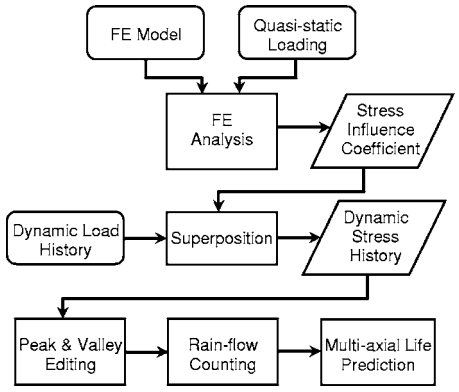

Fig. 3 Flow chart for fatigue life prediction

life, because the primary concern is not the base material, but the fabricated joints; that is, the weld joints. Since the stress state is not uniaxial, the critical plane algorithm is used to convert it to uniaxial fatigue data. In addition, the Goodman model is used to compensate the effect of non-zero mean stress.

From superposition of quasi-static linear finite element analysis and dynamic loading, the stress data are calculated for each element. This stress can be regarded as "true stress," which means if the *S-N* curve for the material is available, it can be applied directly in the fatigue life calculation using the principal stress life method without considering the stress concentration factor. The *S-N* curve can be interpolated from nominal stress-life data of the material, as shown in Fig. 4 for our specific application. The design goal is to maintain the operation for 60,000 h. Since load data are measured for 40 min, this corresponds to about 78,000 cycles.

4 Reliability Analysis and Probability Sensitivity

In general, if the inputs of a system have a probabilistic distribution, the output or response shows a probabilistic behavior as well. In such a case, the safety of the structure cannot be measured with the deterministic value of the response. Rather, the probability that the response is less than the capacity of the system needs to be considered. In reliability analysis, the random inputs are given in an n-dimensional vector $\mathbf{X}$ with a joint probability distribution function (PDF) $f_{\mathbf{X}}(\mathbf{x})$. The state of the system has a Boolean description such that the structure fails when the limit

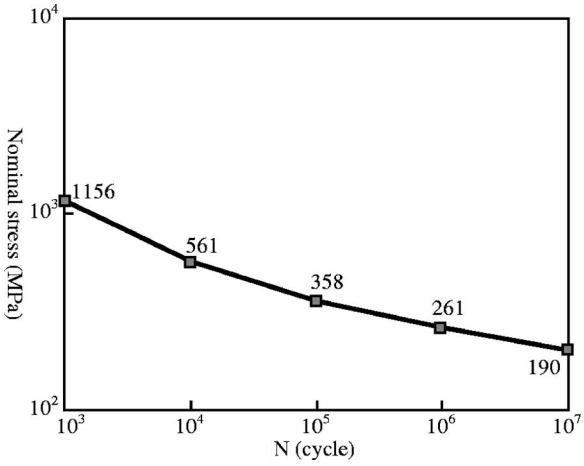

Fig. 4 Stress-based *S-N* curve for the material

Table 1 The type of polynomials and corresponding random variables for different Askey chaos

Random variable	Orthogonal polynomials	Support range
Gaussian	Hermite	$(-\infty, \infty)$
Gamma	Laguerre	$[0, \infty)$
Beta	Jacobi	[a, b]
Uniform	Legendre	[a, b]

state $G(\mathbf{X})$ is less than zero. The probability of failure P_f can be computed as a cumulative distribution function (CDF) over the failed region as

$$P_f = \int_{G(\mathbf{x}) \leqslant 0} f_{\mathbf{X}}(\mathbf{x}) d\mathbf{x} \tag{2}$$

Since the failed region is in general implicit and complex, the reliability integral in Eq. (2) is often performed using the Monte Carlo simulation (MCS) or approximation methods (e.g., first-order reliability method (FORM), or second-order reliability method). In practice, the reliability level of a structure is usually represented by the reliability index $\beta = -\Phi^{-1}(P_f)$ with $\Phi(\cdot)$ being the CDF of the standard normal random variable.

The computational cost of reliability analysis increases exponentially with the number of parameters, without mentioning the cost related to the load tolerance analysis. It appears that the only practical remedy for the computational cost is to construct a response surface and perform reliability analysis using it. In this paper, a stochastic response surface method [2] is used to predict the relationship between the fatigue life and load capacity coefficients in the standard Gaussian space. The stochastic response surface is a particular family of polynomial chaos expansions [10,11] using orthogonal polynomials. Orthogonal polynomials have many useful properties in the solution of mathematical and physical problems. Just as Fourier series provide a convenient method of expanding a periodic function in a series of linearly independent terms, orthogonal polynomials provide a natural way to solve, expand, and interpret solutions to different types of differential equations. Orthogonal polynomials associated with the generalized polynomial chaos (Askey chaos) [11] are different according to the different weight functions. The type of polynomials is decided by the match between the specific weight function and the standard probability density function (PDF). The types of polynomials and their associated random variables [12] with various PDFs are listed in Table 1.

In Table 1, for example, Hermite polynomial bases are orthogonal [13] when the Gaussian PDF is used as a weight function. Thus, the following property holds:

$$\int_{\Omega_u} \varphi(u) \Gamma_i(u) \Gamma_j(u) du = C \delta_{ij}, \quad \forall\, i,j \tag{3}$$

where $\varphi(u)$ is the Gaussian PDF and $\Gamma_i(u)$ is the ith order Hermite polynomial bases.

The stochastic response surface based on the polynomial chaos expansion can be viewed as an extension of classical deterministic response surfaces [14–16], which are constructed using uncertain inputs and performance data collected at heuristically selected collocation points. Let n be the number of random variables and p the order of polynomial. The model output G^p can then be expressed in terms of standard random variables $\{u_i\}$ as

$$G^p = a_0^p + \sum_{i=1}^{n} a_i^p \Gamma_1(u_i) + \sum_{i=1}^{n} \sum_{j=1}^{i} a_{ij}^p \Gamma_2(u_i, u_j) + \sum_{i=1}^{n} \sum_{j=1}^{i} \sum_{k=1}^{j} a_{ijk}^p \Gamma_3(u_i, u_j, u_k) + \ldots \tag{4}$$

where $a_i^p, a_{ij}^p, \ldots$ are deterministic coefficients to be estimated, and $\Gamma_p(u_i, \ldots, u_p)$ are multi-dimensional Hermite polynomials [17] of degree p given by

$$\Gamma_p(u_i, \ldots, u_p) = (-1)^p e^{1/2\mathbf{u}^T\mathbf{u}} \frac{\partial^p}{\partial u_i \ldots \partial u_p} e^{-1/2\mathbf{u}^T\mathbf{u}} \tag{5}$$

where $\mathbf{u}$ is a vector of p independent and identically distributed normal random variables selected among the n random variables that represent the input uncertainties. In this paper, a modified version of the Hermite polynomial [13] is used. The first four terms are u, u^2-1, u^3-3u, u^4-6u^2+3, when a single random variable is involved. The use of the Hermite polynomials has two purposes: (1) they are used to determine the sampling points, and (2) they are used as bases for polynomial approximation.

In general, the approximation accuracy increases with the order of the polynomial, which should be selected by reflecting accuracy and computational constraints. The Hermite polynomials, which are orthogonal with respect to the Gaussian measure, provide approximation with attractive features, namely: more robust estimates of the coefficients with respect to those obtained using non-orthogonal polynomials [18]. They converge to any process with finite second-order moments [19], and the convergence is optimal (exponential) for Gaussian processes [11]. Some numerical examples of the accuracy and convergence of the stochastic response surface in the application of structural design can be found in Kim et al. [20].

The coefficients in the polynomial chaos expansion are calculated as those providing the best fit (least squares solution) considering a sample of input/output pairs. Since all inputs are represented using standard normal random variables, more accurate estimates for the coefficients can be expected if the probability distribution of the u_i's are considered. The idea of Gaussian quadrature of a numerical integral can be borrowed to generate collocation points [17]. In Gaussian quadrature, the function arguments are given by the roots of the next higher-order polynomial. Similarly, the roots of the next higher-order polynomial are used as the points where the approximation is being solved, which is proposed as an orthogonal collocation method by Villadsen and Michelsen [17,21].

For example, to solve for a three-dimensional second-order polynomial chaos expansion, the roots of the third-order Hermite polynomial, $-\sqrt{3}$, 0 and $\sqrt{3}$, are used; thus the possible collocation points are (0, 0, 0), $(-\sqrt{3},-\sqrt{3},-\sqrt{3})$, $(-\sqrt{3}, 0, -\sqrt{3})$, etc. There are 27 possible collocation points. However, from Eq. (4), there are only 10 unknowns. Similarly, for higher-dimensional systems and higher-order approximations, the number of available collocation points is always greater than the number of unknowns, which introduces the problem of selecting the appropriate collocation points. The choice of collocation points is critical for a good approximation. Hence, a set of points near the high probability region is heuristically selected among the roots of the one-order higher polynomial under restrictions of symmetry and proximity to the mean [20]. Since the origin always corresponds to the highest probability in standard Gaussian space, the exclusion of the origin as a collocation point could potentially lead to a poor estimation. Thus, in addition to the standard orthogonal collocation method, a modification of including zero into the roots of the one-order higher polynomial, is made in case there is no zero in these roots.

When the number of random variables increases, the stochastic response surface encounters difficulty due to the curse of dimen-

Table 2 Accuracy of sampling-based sensitivity analysis

Distribution type	Performance	FORM	MCS on SRS (10^5 samples)	Exact
Normal	P_f	0.0915	0.0914	0.0915
$(0, 0.4^2)$	$\partial P^f/\partial\mu$	0.4100	0.4109	0.4100
Lognormal	P_f	0.3287	0.3287	0.3287
$(0.5, 0.4^2)$	$\partial P^f/\partial\mu$	1.1757	1.1763	1.1765
Uniform	P_f	0.1555	0.1556	0.1556 (7/45)
$(-2, 1)$	$\partial P^f/\partial\mu$	0.3334	0.3333	0.3333 (1/3)

sionality. This is true for all response surface-based approaches. There are two possible remedies for this difficulty. The first is to use the local sensitivity information in constructing the response surface, as presented by Kim et al. [20]. The second is to reduce the number of random variables. In many practical cases, only a handful of random variables significantly contributes to the variability of the output. In such a case, those random variables whose contribution to the output variability is small can be considered as deterministic variables and be fixed at their mean value. For that purpose, Kim et al. [22] used the global sensitivity index to identify the contribution of input random variables to the variability of the output. By utilizing the local and the global sensitivity information, the required number of analyses can be significantly reduced.

In this paper, the fatigue life of a structural part is considered as a model output. However, the range of the model output changes over several orders of magnitude. Accordingly, logarithmic fatigue life is approximated using the stochastic response surface in Eq. (4). Reliability analysis is then carried out by the Monte Carlo simulation (MCS) [23,24] operated on the stochastic response surface. In MCS, the probability of failure is calculated by

$$P_f = \int_{\Omega_{\mathbf{x}}} I(G(\mathbf{x}) \leqslant 0) f_{\mathbf{X}}(\mathbf{x}) d\mathbf{x} \tag{6}$$

where $G(\mathbf{x}) \leqslant 0$ is the failure region, $f_{\mathbf{X}}(\cdot)$ the joint probability density function, and $I(G(\mathbf{x}) \leqslant 0)$ the indication function in such a way that $I=1$ if $G(\mathbf{x}) \leqslant 0$ and $I=0$ otherwise. In Eq. (6), $\Omega_{\mathbf{x}}$ denotes the entire random design space. In the stochastic response surface, however, all input random variables are transformed into the standard random variable space $\Omega_{\mathbf{u}}$. Since the explicit expression of the model output is given in terms of Hermite polynomial bases as in Eq. (4), MCS is inexpensive even with 10^5 samples.

In estimating the safety envelope, the sensitivity information plays an important role. When moment-based methods are used, the sensitivity of the reliability index can be calculated without requiring additional computation. However, sensitivity calculation in sampling-based methods, such as in Eq. (6), is not trivial due to the uncertainty involved in the Monte Carlo integral. Let θ be a statistical parameter. Then, the sensitivity of failure probability can be obtained by following a similar Monte Carlo integral as

$$\frac{\partial P_f}{\partial \theta} = \int_{\Omega_{\mathbf{u}}} \left\{ I(G(\mathbf{x}) \leqslant 0) \left[\frac{\partial f_{\mathbf{X}}(\mathbf{x})}{f_{\mathbf{X}}(\mathbf{x}) \partial \theta} \right]_{\mathbf{x}=\mathbf{T}^{-1}(\mathbf{u})} \varphi(\mathbf{u}) \right\} d\mathbf{u} \tag{7}$$

where $\varphi(\mathbf{u})$ is the joint PDF of standard normal random variables. Using the relation between the probability of failure and the reliability index, the sensitivity of the reliability index can be obtained as

$$\frac{\partial \beta}{\partial \theta} = -\frac{1}{\varphi(-\beta)} \frac{\partial P_f}{\partial \theta} \tag{8}$$

Detailed expressions of $\partial P_f/\partial\theta$ for different distribution types are summarized in the Appendix. When the input variable is normally distributed, sensitivity with respect to random parameters in Eq. (7) can be obtained from Eq. (A1).

As an illustration of the accuracy of sampling-based probability sensitivity analysis, consider a simple linear analytical function $G(X)=1.6-3X$, with X being a random variable. Three different distribution types are considered. The accuracy of the sampling-based sensitivity calculation in the above equations can be evaluated by comparing it with the sensitivity from the first-order reliability method (FORM) [25–27] or from the exact solution. When the function is linear and the input is normally distributed, the reliability and its sensitivity from FORM will yield the exact values. Table 2 compares the probability of failure and its sensitivity with respect to random parameters. The proposed sensitivity calculation results agree with those from FORM [28] and the exact solution.

5 Estimation of the Load Tolerance Using Sensitivity

First, a single parameter is selected to estimate the load tolerance of the structure using sensitivity information. Suppose the average value of the dynamic load remains constant, while the amplitude changes randomly. From Eq. (1), the uncertainty of the amplitude can be represented using the following parametrization of the dynamic load:

$$f(t) = f_{\text{ave}} + \gamma(f_0(t) - f_{\text{ave}}) \tag{9}$$

When $\gamma=1$, we can recover the original load history. When $\gamma=0$, the dynamic load becomes a static one with the average value. In this definition, γ cannot take a negative value.

Since accurate information is unavailable for the dynamic load and also many uncertainties are involved, the load capacity coefficient (LCC) γ is defined as a random variable with normal distribution: ($\mu_\gamma=1$ and $\sigma_\gamma=0.25$). The standard deviation of γ is obtained from the coefficient of variance of the measured load data $f_0(t)$. This distribution type will be compared with the lognormal distribution in the following section.

For other types of random variables, an appropriate transformation must be employed. Devroye [29] presents the required transformation techniques and approximations for a variety of probability distributions. More arbitrary probability distributions can be approximated using algebraic manipulations or by series expansions.

The random variable γ can be converted into the standard normal random variable u by

$$u = \frac{\gamma - \mu_\gamma}{\sigma_\gamma} \tag{10}$$

where $u \sim N(0, 1^2)$. In order to see the effect of the mean change, we further fix the standard deviation. Thus, the only variable is the mean value of the random variable γ. The goal is to find the value of μ_γ, the point where the structure fails.

For any given sample point u, a corresponding γ can be obtained from Eq. (10), and using γ, a new dynamic load history can be obtained from Eq. (9). By applying this dynamic load history, we can calculate the fatigue life of the structure. Since this procedure includes multiple steps, we can construct a stochastic response surface for the fatigue life and then perform the reliability analysis using the stochastic response surface. Since the fatigue

Table 3 Error measures of the stochastic response surface

Error statistics	RMSE	SS_e	R^2	R^2_{adj}
DOE	0.0406	0.0082	0.9980	0.9921

Table 4 T statistics for the estimation of coefficients

Coefficient	1	u	u^2-1	u^3-3u
T statistics	122.7590	15.9279	3.5759	4.0828

life changes by several orders of magnitude, we construct the stochastic response surface for the logarithmic fatigue life. We construct a cubic stochastic response surface as a surrogate model for the logarithmic fatigue life as

$$L(\gamma(u)) = \log_{10}(\text{Life}) = 5.7075 - 0.7223u - 0.0581(u^2 - 1) + 0.0756(u^3 - 3u) \quad (11)$$

The above response surface shows that the mean of the logarithmic fatigue life is 5.7075 and the standard deviation is about 0.7223. It also shows that the contribution of the higher-order terms is relatively small compared to the constant and linear terms. Thus, we can conclude that the performance is mildly nonlinear with respect to the random variable. The accuracy of the stochastic response surface is evaluated using the various statistical error measures in Tables 3 and 4, which show the good quality of the approximation.

For a given logarithmic target life L_{target} (=60,000 h), the structure is considered failed when the predicted life in Eq. (11) is less than the target life. Accordingly, we can define the probability of failure as

$$P_f := P[L(\gamma) - L_{target} \leqslant 0] \leqslant P_{target} \quad (12)$$

where P_{target} is the target probability of failure. For example, when $P_{target}=0.1$, the probability of failure should be less than 10%. Even though the interpretation of Eq. (12) is clear, it is often inconvenient because the probability changes by several orders of magnitude. In reliability analysis, it is more common to use the reliability index, which uses the notion of the standard normal distribution. Equation (12) can be rewritten in terms of the reliability index as

$$\Phi(-\beta) := P_f \leqslant P_{target} := \Phi(-\beta_{target}) \quad (13)$$

When $P_{target}=0.1$, $\beta_{target} \approx 1.3$. The advantage of using the reliability index will be clear in the following numerical results.

Using the response surface in Eq. (11), reliability analysis is carried out using the first-order reliability method (FORM) at $\mu_\gamma=1$. The results of the reliability analysis are as follows:

$$P_f = 0.178$$
$$\beta = 0.922, \quad (14)$$
$$\frac{\partial \beta}{\partial \mu_\gamma} = -3.972$$

where $\partial\beta/\partial\mu_\gamma$ is the sensitivity of the reliability index with respect to μ_γ. By comparing this with the target reliability, the current system does not satisfy the reliability requirement.

It is obvious that for a linear and deterministic system, the response is linear with respect to the applied load. Thus, estimating the load tolerance is trivial. However, the fatigue reliability of the structure is not linear with respect to the applied load history. When the fatigue reliability is mildly nonlinear, it is still possible to estimate the safety envelope using sensitivity information. Based on the result from Eq. (14), the value of μ_γ that satisfies the required reliability can be estimated using a linear approximation. The linear estimation of μ_γ can be obtained by

$$\mu_\gamma^{\text{estimated}} = 1 - \frac{(\beta_{\mu_\gamma=1} - \beta_{target})}{\dfrac{\partial \beta_{\mu_\gamma=1}}{\partial \mu_\gamma}} = 0.905 \quad (15)$$

which means that μ_γ needs to be decreased by 10% from the original load amplitude in order to satisfy the required reliability.

In order to verify the accuracy of the estimated result, reliability analyses are performed for different values of μ_γ. Figure 5 shows the reliability index with respect to μ_γ, while Fig. 6 shows the probability of failure P_f with respect to μ_γ. The solid line is the linearly approximated reliability using the sensitivity information, and the triangular marks are the results from the direct reliability analyses. The reliability index is almost linear and the estimation using sensitivity is close to the actual reliability index. Such an interesting result is expected, because the amplitude parameter is normally distributed and the reliability index is based on the standard normal distribution. On the other hand, the probability of

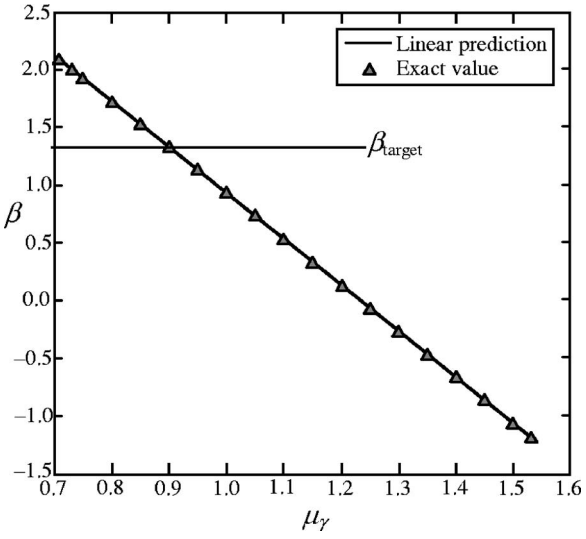

Fig. 5 Reliability index β with respect to random variable μ_γ

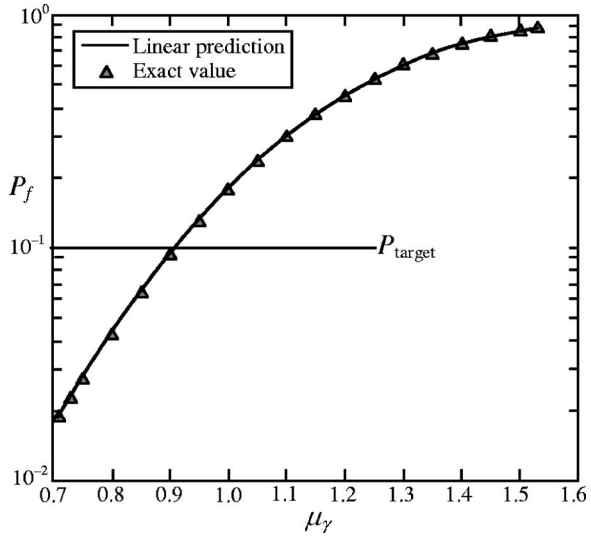

Fig. 6 Probability of failure P_f with respect to random variable μ_γ

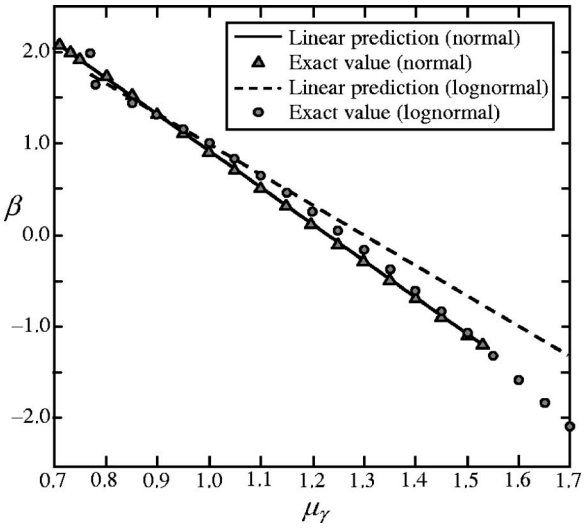

Fig. 7 Reliability index β with respect to μ_γ for both normal and lognormal distributions with the same parameters

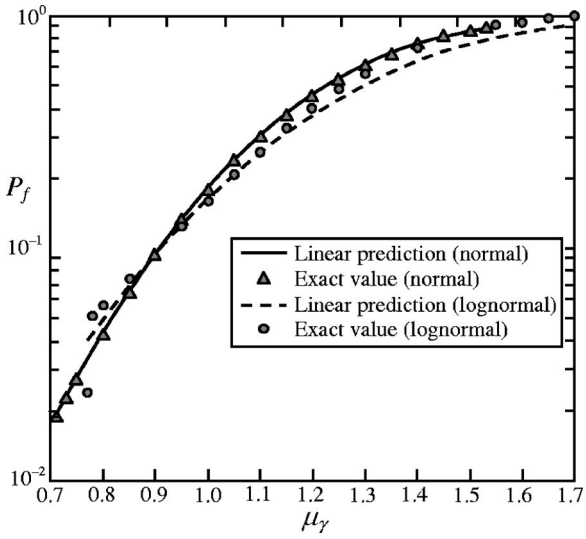

Fig. 8 Probability of failure P_f with respect to μ_γ for both normal and lognormal distributions with the same parameters

failure shows nonlinear behavior even in the logarithmic scale because its magnitude changes by several orders of magnitude.

When the target probability of failure is 0.1 and γ has the distribution of $N(\mu_\gamma, 0.25^2)$, the load tolerance can be defined as

$$0 \leqslant \mu_\gamma \leqslant 0.9049 \tag{16}$$

Thus, the current design, considering the 0.25 standard deviation in the load amplitude, is not enough to achieve 90% reliability. The structure should be operated under milder working conditions by reducing the mean of the load amplitude by about 10%. The predicted load tolerance shows a good agreement with the actually calculated load tolerances (triangular marks). These results are promising in estimating the load-carrying capability of the structure.

6 Effect of Different Distribution Types on Load Tolerance and a Conservative Distribution Type

In the previous section, we assumed that the load history had specific uncertainty characteristics (distribution type and corresponding parameters). Identifying the load distribution, however, is one of the most difficult tasks in uncertainty analysis, because different operating conditions may yield completely different distribution types. Instead of identifying uncertainty distribution accurately, design engineers often look for a conservative distribution type. Figures 7 and 8 show the difference between normal and lognormal distributions. Note that lognormal distribution shows higher nonlinearity in the relation of reliability indices and the mean of LCC. The linear prediction of load tolerance for lognormal LCC cannot be accurate enough, but it is still possible to apply piecewise linear prediction to the load tolerance design by restricting the step size to an acceptable range. The lognormal distribution is more conservative when the amplitude of the applied load is small, whereas normal distribution is more conservative when the amplitude is large. Using sensitivity and linear approximation, it is possible to predict which distribution type has a significant effect on the load tolerance. Once a dominant distribution type is selected, the detailed load tolerance can be constructed by following the procedure explained in the previous section.

7 Multi-Dimensional Safety Envelope

When more than one parameter is involved in load tolerance estimation, the safe region of the parameters constitutes a closed, multi-dimensional domain. The boundary of the domain is called the safety envelope. For illustration purposes, consider two parameters, α and γ. When the two parameters are gradually increased from zero, the initially safe structure becomes unsafe at certain values of the parameters. Due to the property of a truncated cone, a single failure boundary can be found when two parameters are increased proportionally. If all combinations of the parameter values that make the structure unsafe are connected, a closed envelope can be constructed. Figure 9 shows a schematic illustration of the safety envelope when two parameters are involved. However, searching for all possible values of parameters is time consuming and, in many applications, impractical. The technical challenge is how to find the boundary of the envelope without using the trial-and-error approach.

In this paper, a systematic way of searching the boundary of the safety envelope is proposed using a predictor-corrector method, which is similar to the Euler-Newton continuation method [30]. When the relationship between the safety of the structure and the applied loads is linear or mildly nonlinear, this approach can produce an efficient way of estimating the safety envelope. In the context of reliability-based safety measure, the boundary of the safety envelope is the location where the probability of failure is equal to the target probability.

The predictor-corrector algorithm is explained below with two random variables, α and γ. First, the distribution type of random variables is assumed. The effect of different distribution types on the safety envelope can be investigated by following the same procedure as in the previous section. It is clear that the two parameters must have non-negative values, which means that the safety envelope only exists in the first quadrant. The capacity of

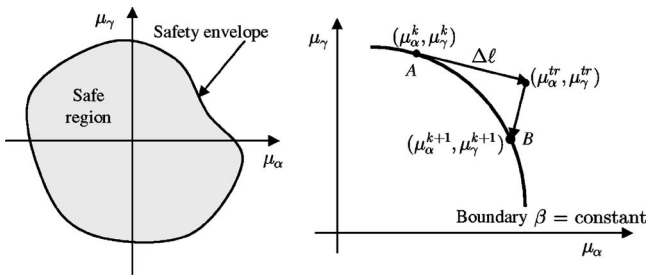

Fig. 9 Safety envelope for two variables and the predictor-corrector algorithm finding the boundary of the envelope. The accuracy can be improved by using a smaller size of move limit $\Delta\ell$.

the structure with respect to (μ_α, μ_γ) is interesting. If the required probability of failure is P_{target} (i.e., $\beta_{\text{target}} = -\Phi^{-1}(P_{\text{target}})$), the following steps can be taken to construct the safety envelope:

1. Set $k=1$. Set the move limit $\Delta\ell$ and a small parameter ε. Initialize $(\mu_\alpha, \mu_\gamma) = (\mu_\alpha^0, \mu_\gamma^0)$.
2. Find an initial state $(\mu_\alpha^1, \mu_\gamma^1)$ such that $\beta(\mu_\alpha^1, \mu_\gamma^1) = \beta_{\text{target}}$.
   The initial state can be found, for example, by fixing $\mu_\alpha^1 = \mu_\alpha^0$ and searching μ_γ^1 as described in the previous sections.
3. Determine the trial state (predictor).
   The trial state can be obtained by moving in the tangent direction of the boundary of the envelope. From the first-order Taylor series expansion of $\beta(\mu_\alpha^k, \mu_\gamma^k) = \text{constant}$ and from the move limit of $\Delta\ell$, the following two conditions can be used to determine the trial increments:

$$(\Delta\mu_\alpha^{tr})^2 + (\Delta\mu_\gamma^{tr})^2 = \Delta\ell^2 \tag{17}$$

$$\left.\frac{\partial\beta}{\partial\mu_\alpha}\right|_{\mu_\alpha=\mu_\alpha^k} \cdot \Delta\mu_\alpha^{tr} + \left.\frac{\partial\beta}{\partial\mu_\gamma}\right|_{\mu_\gamma=\mu_\gamma^k} \cdot \Delta\mu_\gamma^{tr} = 0 \tag{18}$$

   Of the two possible directions, the one that provides a clockwise (or counterclockwise) direction is selected. Then, the trial state can be obtained by

$$\mu_\alpha^{tr} = \mu_\alpha^k + \Delta\mu_\alpha^{tr}$$

$$\mu_\gamma^{tr} = \mu_\gamma^k + \Delta\mu_\gamma^{tr} \tag{19}$$

   According to the convex property of the envelope, the trial state in Eq. (19) can be either inside or outside the envelope. The reliability index at the trial state is $\beta^{tr} = \beta(\mu_\alpha^{tr}, \mu_\gamma^{tr})$.
4. Return to the boundary of the envelope (corrector).
   Since the trial state is not on the boundary, it needs to be returned to the boundary of the envelope. The correcting direction is perpendicular to the trial direction.

$$\beta_{\text{target}} = \beta^{tr} + \left.\frac{\partial\beta}{\partial\mu_\alpha}\right|_{\mu_\alpha=\mu_\alpha^{tr}} \cdot \Delta\mu_\alpha^{cr} + \left.\frac{\partial\beta}{\partial\mu_\gamma}\right|_{\mu_\gamma=\mu_\gamma^{tr}} \cdot \Delta\mu_\gamma^{cr} \tag{20}$$

$$\Delta\mu_\alpha^{cr} \cdot \Delta\mu_\alpha^{tr} + \Delta\mu_\gamma^{cr} \cdot \Delta\mu_\gamma^{tr} = 0 \tag{21}$$

   Then, the new state on the boundary of the envelope can be obtained by

$$\mu_\alpha^{k+1} = \mu_\alpha^{pr} + \Delta\mu_\alpha^{cr}$$

$$\mu_\gamma^{k+1} = \mu_\gamma^{pr} + \Delta\mu_\gamma^{cr} \tag{22}$$

5. Stop if $\|(\mu_\alpha^{k+1}, \mu_\gamma^{k+1}) - (\mu_\alpha^1, \mu_\gamma^1)\| \leq \varepsilon$.
6. Otherwise, set $k=k+1$ and go to Step 3.

As schematically explained in Fig. 9, the limit of the envelope is first found in one parameter μ_α, while μ_γ is fixed (Point A). The reliability result and sensitivity information are calculated at this point, from which the new search direction is found using sensitivity information and linear Taylor series expansion. The trial state can be obtained by moving the parameters by $\Delta\ell$ in the search direction. From the trial state, the location of the boundary can be recovered by moving in the perpendicular direction to the search direction. Using the linear search, a new position B on the envelope can be found. This sequence can be repeated to create a closed safety envelope. As expected, the accuracy of the safety envelope can be improved by using a smaller size of move limit. This safety envelope provides important information in identifying a capacity of the current design, a future reference for design upgrade, maintenance and control, etc.

Figure 10 shows the two-dimensional safety envelope for the civil construction equipment when both parameters are normally distributed. As discussed before, the safety envelope is defined only on the first quadrant because both parameters are positive. It is clear from the figure that the structure has a larger safety margin in the average value than that of the amplitude. In fact, the structure is not safe with the initial dynamic load amplitude. This observation is consistent with the one-dimensional case study in the previous sections. As expected, the safety envelope satisfies the property of a truncated cone such that it fails only once if the mean values of the parameters are increased proportionally from the origin. In addition, the boundary of the safety envelope shows a mild non-linear variation.

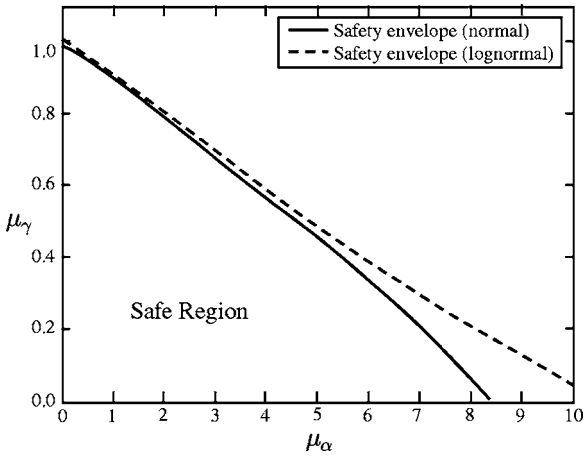

Fig. 10 Two-dimensional safety envelope of fatigue reliability for different distribution types with the same random parameters. The normal distribution shows more conservative estimation than lognormal distribution.

Figure 10 also shows the safety envelope when the two parameters have a lognormal distribution with the same random parameters, i.e., mean and standard deviation. This information is useful because in many cases the random parameters are identified, but the distribution type is unclear. In such a case, the different distribution types are assumed and the conservative safety envelope can be selected. In the particular example, it turns out that the normal distribution is more conservative than the lognormal distribution. In some cases, it is possible that one distribution type is more conservative than the other only on a portion of the safety envelope. Thus, a conservative safety envelope can be constructed by considering all possible distribution types associated with different working conditions. The completed safety envelope yields a more reliable operation and provides a reference for future design upgrades.

8 Conclusion

In this paper, a systematic road map of constructing the safety envelope has been presented. Finite element-based fatigue evaluation, stochastic response surface-based reliability and sensitivity analysis, and a predictor-corrector algorithm are integrated to construct a design reference for a structure. Accuracy and robustness of the sampling-based probability sensitivity analysis has been shown through a simple numerical example. For one-dimensional problems, it is shown that the load tolerance can be estimated using a sensitivity of the reliability index. The conservative distribution type is considered to offer a safer design of load without complete knowledge of uncertainty properties. The procedure of safety envelope construction has been presented by introducing a two-dimensional uncertainty model for load tolerance estimation. When the safety is mildly nonlinear with respect to the random parameters, the proposed approach provides a very efficient way of constructing the safety envelope. Complete work has been done by constructing a multi-dimensional safety envelope for load tolerance with investigation of the conservative distribution type.

Acknowledgment

We would like to thank Professor B. M. Kwak for valuable suggestions and discussions.

Appendix: Probability Sensitivity for Various Distribution Types

In this section, the detailed sampling-based sensitivity expressions in Eq. (7) are presented for different distribution types. The expression of the normally distributed variable is available in Wu [4]. Other distribution types can be derived based on their probability distribution function and transformation to the standard normal random variable.

1. Normally distributed variables

$$\frac{\partial P_f}{\partial \mu} = \frac{1}{N}\sum_{j=1}^{N} I_j \frac{1}{\sigma_i} u_i^j \tag{A1}$$

$$\frac{\partial P_f}{\partial \sigma} = \frac{1}{N}\sum_{j=1}^{N} I_j \frac{1}{\sigma_i} (u_i^j u_i^j - 1) \tag{A2}$$

2. Lognormally distributed variables

$$\begin{aligned}\frac{\partial P_f}{\partial \mu_i} &= \int_{\Omega_u} I(G(\mathbf{u}) \leqslant 0) \cdot \left[\frac{\partial f(\mathbf{x})}{f(\mathbf{x})\partial \mu_i}\right]_{\mathbf{x}=\mathbf{T}^{-1}(\mathbf{u})} \varphi(\mathbf{u}) d\mathbf{u} \\ &= \frac{1}{N}\sum_{j=1}^{N}\left[\frac{\ln(x_i^j) - \tilde{\mu}_i}{\tilde{\sigma}_i^2} \cdot \left(\frac{1}{\mu_i} + \frac{v_i}{(\mu_i - a)(1+v_i^2)}\right)\right. \\ &\quad \left. + \frac{v^2}{\tilde{\sigma}_i(\mu - a)(1+v^2)} \cdot \left(\frac{1}{\tilde{\sigma}_i} - \frac{[\ln(x_i^j) - \tilde{\mu}_i]^2}{\tilde{\sigma}_i^3}\right)\right]_{\mathbf{x}=\mathbf{T}^{-1}(\mathbf{u})}\end{aligned} \tag{A3}$$

3. Uniformly distributed variables

The probability density function for uniform distribution is

$$f(x) = \frac{1}{b-a}, \quad a \leqslant x \leqslant b$$

$$\mu = \frac{a+b}{2}, \quad \sigma = \frac{b-a}{\sqrt{12}} \tag{A4}$$

Thus

$$a = \mu - \sqrt{3}\sigma$$

$$b = \mu + \sqrt{3}\sigma$$

Using the step function and the trigonometric function, the uniform distribution function can be rewritten as

$$\begin{aligned} f(x) &= \frac{1}{b-a}[H(x-a) - H(x-b)] \\ &\approx \frac{1}{(b-a)\pi}\{\arctan[c(x-a)] - \arctan[c(x-b)]\} \end{aligned} \tag{A5}$$

where the arc-tangent function is used to approximate the step function into a continuous function for the purpose of derivation. When $c \to \infty$, the right-hand side of Eq. (A5) converges to $f(x)$. For an N-dimensional system, by assuming that all system random variables are independent, the joint probability distribution function is defined as

$$f(\mathbf{x}) = \prod_{i=1}^{N} \frac{1}{(b_i - a_i)\pi}\{\arctan[c(x_i - a_i)] - \arctan[c(x_i - b_i)]\} \tag{A6}$$

The sensitivity of failure probability P_f to the mean of the uniform random variable X_i can be written as

$$\begin{aligned}\frac{\partial P_f}{\partial \mu_i} &= \int_{\Omega_\mathbf{X}} I(G(\mathbf{x}) \leqslant 0) \frac{\partial f(\mathbf{x})}{\partial \mu_i} d\mathbf{x} \\ &= \frac{c}{N}\sum_{j=1}^{N}\left\{\frac{\frac{1}{1+c^2(x_i^j - b_i)^2} - \frac{1}{1+c^2(x_i^j - a_i)^2}}{\arctan[c(x_i^j - a_i)] - \arctan[c(x_i^j - b_i)]}\right\}_{\mathbf{x}=\mathbf{T}^{-1}(\mathbf{u})}\end{aligned} \tag{A7}$$

Nomenclature

f	=	load history
G	=	system response
α, γ	=	load capacity coefficients
β	=	reliability index
P_f	=	probability of failure
μ	=	mean
σ	=	standard deviation
T	=	transformation from any random space to standard normal space
u	=	standard normal random variable
L	=	logarithmic fatigue life
Γ_p	=	multi-dimensional Hermite polynomials of degree p
a	=	polynomial coefficient
Ω_u	=	standard normal space
Ω_x	=	random space
FORM	=	first-order reliability method
MCS	=	Monte Carlo simulation
LCC	=	load capacity coefficient
DOF	=	degree of freedom

References

[1] Kwak, B. M., and Kim, J. H., 2002, "Concept of Allowable Load Set and Its Application for Evaluation of Structural Integrity," Mech. Struct. Mach., **30**(2), pp. 213–247.
[2] Isukapalli, S. S., Roy, A., and Georgopoulos, P. G., 2000, "Efficient Sensitivity/Uncertainty Analysis Using the Combined Stochastic Response Surface Method and Automated Differentiation: Application to Environmental and Biological Systems," Risk Anal., **20**(5), pp. 591–602.
[3] Isukapalli, S. S., Roy, A., and Georgopoulos, P. G., 1998, "Stochastic Response Surface Methods (SRSMs) for Uncertainty Propagation: Application to Environmental and Biological Systems," Risk Anal., **18**(3), pp. 351–363.
[4] Wu, Y.-T., 1994, "Computational Methods for Efficient Structural Reliability and Reliability Sensitivity Analysis," AIAA J., **32**(8), pp. 1717–1723.
[5] Liu, H., Chen, W., and Sudjianto, A., 2004, "Probability Sensitivity Analysis Methods for Design under Uncertainty," *Tenth AIAA/ISSMO Multidisciplinary Analysis and Optimization Conference*, Albany, NY., August 30-September 1.
[6] Safe Technology, 2004, FE-SAFE, Software Package, Ver. 5.1, Sheffield, England.
[7] Yu, X. M., Chang, K. H., and Choi, K. K., 1998, "Probabilistic Structural Durability Prediction," AIAA J., **36**(4), pp. 628–637.
[8] Matsuishi, M., and Endo, T., 1968, "Fatigue of Metals Subjected to Varying Stress-Fatigue Lives Under Random Loading," *Proceedings of the Kyushu District Meeting*, JSEM, Fukuoka, Japan, pp. 37–40.
[9] Miner, M. A., 1945, "Cumulative Damage in Fatigue," J. Appl. Mech., **12**, pp. A159–A164.
[10] Ghanem, R. G., and Spanos, P. D., 1991, *Stochastic Finite Elements: A Spectral Approach*, Springer-Verlag, New York.
[11] Xiu, D., Lucor, D., Su., C.-H., and Karniadakis, G. E., 2002, "Stochastic Modeling of Flow-Structure Interactions Using Generalized Polynomial Chaos," J. Fluids Eng., **124**(1), pp. 51–59.
[12] Choi, S. K., Grandhi, R. V., Canfield, R. A., and Pettit, C. L., 2003, "Polynomial Chaos Expansion With Latin Hypercube Sampling for Predicting Response Variability," *44th AIAA/ASME/ASCE/AHS Structures, Structural Dynamics, and Materials Conference*, Norfolk, VA, April 7-10.
[13] Abramowitz, M., and Stegun, I. A., 1972, "Orthogonal Polynomials," *Hand-*

book of Mathematical Functions With Formulas, Graphs, and Mathematical Tables, 9th ed., Dover, New York, pp. 771–802.
[14] Myers, R. H., and Montgomery, D. C., 1995, *Response Surface Methodology: Process and Product Optimization Using Designed Experiments*, Wiley, New York.
[15] Khuri, A. I., and Cornell, J. A., 1996, *Response Surface: Design and Analysis*, Dekker, New York.
[16] Wang, G., 2003, "Adaptive Response Surface Method Using Inherited Latin Hypercube Design Points," ASME J. Mech. Des., **125**(2), pp. 210–220.
[17] Villadsen, J., and Michelsen, M. L., 1978, *Solution of Differential Equation Models by Polynomial Approximation*, Prentice–Hall, Englewood Cliffs, NJ.
[18] Gautschi, W., 1996, *Orthogonal Polynomials: Applications and Computation, Acta Numerica*, Cambridge University Press, Cambridge, pp. 45–119.
[19] Cameron, R. H., and Martin, W. T., 1947, "The Orthogonal Development of Nonlinear Functionals in Series of Fourier-Hermite Functionals," Ann. Math., **48**, pp. 385–392.
[20] Kim, N. H., Wang, H., and Queipo, N. V., 2006, "Efficient Shape Optimization Under Uncertainty Using Polynomial Chaos Expansions and Local Sensitivities," AIAA J., **44**(5), pp. 1112–1116.
[21] Webster, M. D., Tatang, M. A., and McRae, G. J., 1996, "Application of the Probabilistic Collocation Method for an Uncertainty Analysis of a Simple Ocean Model," MIT Joint Program on the Science and Policy of Global Change.
[22] Kim, N. H., Wang, H., and Queipo, N. V., 2005, "Adaptive Reduction of Design Variables Using Global Sensitivity in Reliability-Based Optimization," Int. J. Reliab. Safety (in press).
[23] Metropolis, N., and Ulam, S., 1949, "The Monte Carlo Method." J. Am. Stat. Assoc., **44**(247), pp. 335–341.
[24] Rubinstein, R. Y., 1981, *Simulation and the Monte Carlo Method*, Wiley, New York.
[25] Hasofer, A. M., and Lind, N. C., 1974, "Exact and Invariant Second-Moment Code Format." J. Eng. Mech., **100**(1), pp. 111–121.
[26] Rackwitz, R., 2000, "Reliability Analysis-Past, Present and Future." *Eighth ASCE Specialty Conference on Probabilistic Mechanics and Structure Reliability*, Notre Dame, IN, July 24-26.
[27] Chiralaksanakul, A., and Mahadevan, S., 2005. "First-Order Approximation Methods in Reliability-Based Design Optimization," ASME J. Mech. Des., **127**(5), pp. 851–857.
[28] Karamchandani, A., and Cornell, C. A., 1992, "Sensitivity Estimation Within First and Second Order Reliability Methods," Struct. Safety, **11**, pp. 95–107.
[29] Devroye, L., 1986, *Nonuniform Random Variate Generation*, Springer-Verlag, New York.
[30] Allgower, E. L., and Georg, K., 1990, *Numerical Continuation Methods: An Introduction*, Springer-Verlag, Berlin.